NRC Research and/or Technical Assistance Rept

PDR

EGG-NTAP-6148

December 1982

SCDAP REPLICATION OF MARCH HYDROGEN CALCULATIONS

Rosanna Chambers

Idaho National Engineering Laboratory
Operated by the U.S. Department of Energy

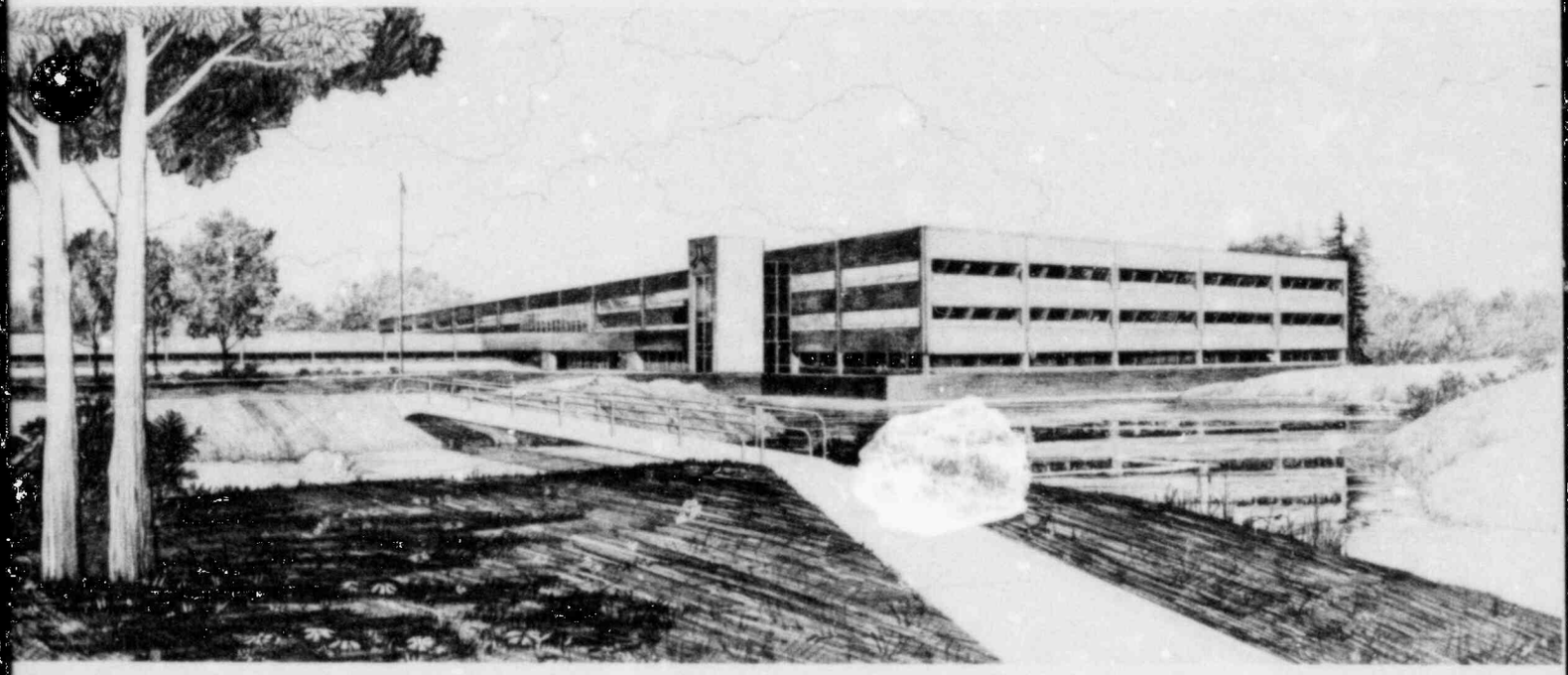

This is an informal report intended for use as a preliminary or working document

Prepared for the
U.S. NUCLEAR REGULATORY COMMISSION
Under DOE Contract No. DE-AC07-76ID01570
NRC FIN No. A6354

EG&G Idaho

EG&G Idaho, Inc.

FORM EG&G-398
(Rev. 03-82)

INTERIM REPORT

Accession No. _____

Report No. EGG-NTAP-6148

Contract Program or Project Title: NRC Technical Assistance Program Division

Subject of this Document: SCDAP Replication of MARCH Hydrogen Calculations

Type of Document: Technical Report

Author(s): Rosanna Chambers

Date of Document: December 1982

Responsible NRC Individual and NRC Office or Division: J. T. Larkins

This document was prepared primarily for preliminary or internal use. It has not received full review and approval. Since there may be substantive changes, this document should not be considered final.

EG&G Idaho, Inc.
Idaho Falls, Idaho 83415

Prepared for the
U.S. Nuclear Regulatory Commission
Washington, D.C.
Under DOE Contract No. DE-AC07-76ID01570
NRC FIN No. A6354

INTERIM REPORT

ABSTRACT

Hydrogen generation and hydrogen generation rate calculations using the Meltdown Accident Response Characteristics (MARCH) computer code were replicated using a module of the Severe Core Damage Analysis Package (SCDAP). Accident sequences reflecting the risk dominant and most probable initiating events for core meltdown sequences in which a hydrogen detonation would challenge containment integrity were chosen for the code calculations. Results are discussed for both pressurized water reactors and boiling water reactors. Conclusions are reached reflecting similarities and differences in the codes' modeling. Recommendations are made for use of the results of this study in conjunction with MARCH calculations and for future use of the SCDAP code.

SUMMARY

The United States Nuclear Regulatory Commission has been involved in rulemaking to assure that reactor containments and containment equipment could withstand accidents involving the generation and burn of large amounts of hydrogen. To aid in NRC rulemaking, a series of computer calculations was performed at the Battelle Columbus Laboratories using the Meltdown Accident Response Characteristics (MARCH) computer code, Version 1.1. The purpose was to define an envelope of histories of hydrogen and steam release rates to the containment during degraded core cooling accidents.

A second effort, using the more mechanistic code, Severe Core Damage Analysis Package (SCDAP), was conducted at EG&G Idaho, Inc. The purpose was to replicate these MARCH code calculations in the reactor core area. An early version of the component analysis module of SCDAP was used in this study. This module, designated SCDCOMP, computes the behavior of single fuel rods during severe core disruptions. This task which is summarized in this report, was conducted by the NRC Technical Assistance Program Division of EG&G Idaho Inc., as part of the Severe Accident Sequence Analysis Program.

Sixteen accident scenarios were chosen by the Battelle Columbus Laboratories. These accident scenarios were chosen to be the risk dominant and most probable initiating events for core meltdown sequences in which hydrogen burning is significant. These sequences included small, intermediate, and large break loss-of-coolant accidents and transients with failure of emergency core cooling systems. Some of the sequences modeled a pressurized water reactor with an ice condenser containment and the remainder modeled a boiling water reactor with a Mark-III containment.

Both the SCDCOMP and MARCH codes were used to calculate hydrogen generation and hydrogen generation rates for each of the scenarios. The MARCH code models the entire reactor system while the SCDCOMP code models only

the core region of the reactor. Since the purpose of the study was to repeat the MARCH calculations as closely as possible for only the core region of the reactor, thermal-hydraulic boundary conditions were supplied to the SCDCOMP code from the MARCH code.

The general conclusions from this study are:

1. Hydrogen generation calculations are sensitive to two mechanistic models affecting cladding oxidation that are present in SCDAP but absent in MARCH, Version 1.1.

2. The quantity and rate of hydrogen generation calculated by SCDCOMP is scenario dependent.

3. SCDCOMP is more sensitive than MARCH, Version 1.1 to increased steam flow due to ECC injection.

4. SCDCOMP modelling of fuel rods allows more accurate use of oxidation kinetics models.

Since changes in thermal-hydraulic boundary conditions can significantly affect SCDCOMP calculations, it is recommended that several of the calculations be redone using boundary conditions obtained from a best estimate reactor system code. SCDAP/MODO will contain such a best estimate thermal-hydraulic subcode.

CONTENTS

FIGURES

SCDAP REPLICATION OF MARCH HYDROGEN CALCULATIONS

1. INTRODUCTION

The United States Nuclear Regulatory Commission (NRC) has been concerned with assuring that reactor containments and containment equipment could withstand accidents involving the generation and burn of large amounts of hydrogen. To aid in NRC rulemaking, a series of computer calculations was performed[1] at the Battelle Columbus Laboratories using the Meltdown Accident Response Characteristics (MARCH) computer code,[2] Version 1.1. The purpose was to define an envelope of histories of hydrogen and steam release rates to the containment during degraded core cooling accidents.

A second effort, using the more mechanistic code, Severe Core Damage Analysis Package (SCDAP),[3] was conducted at EG&G Idaho, Inc. The purpose was to replicate these MARCH code calculations in the reactor core area. An early version of the component analysis module of SCDAP was used in this study. This module, designated SCDCOMP, computes the behavior of single fuel rods during severe core disruptions. This task which is summarized in this report, was conducted by the NRC Technical Assistance Program Division of EG&G Idaho Inc., as part of the Severe Accident Sequence Analysis Program.

In this report, an overview of the MARCH and SCDCOMP codes is presented. The procedure used to determine hydrogen generation rates is described, along with the modeling used in the two codes. The results of the SCDCOMP calculations are given and compared with the results from the MARCH calculations. Conclusions and recommendations are presented, as well as a list of references. The Appendix contains a set of plots that detail results from the SCDCOMP and MARCH code calculations.

2. CODE DESCRIPTIONS

The two codes, MARCH and the SCDCOMP module of SCDAP, were used to calculate the rate of hydrogen production during various reactor accidents involving degraded core cooling. A brief description of the MARCH code is given below, followed by a description of SCDCOMP.

2.1 MARCH, Version 1.1

The MARCH computer code describes the response of light water reactor systems to either a small or a large pipe break accident, or an operational transient accident, any of which can result in core meltdown. Calculations are performed during the entire course of the accident including blowdown, core heatup, boiloff, core meltdown, pressure vessel bottom head failure, debris-water interaction in the reactor cavity, and interaction of the molten debris with the concrete base pad. Included in MARCH are models that calculate core temperature, zircaloy oxidation, and hydrogen generation and combustion. MARCH was intended for use in risk analysis for accidents involving core meltdown.

Overall, MARCH uses very simplistic, generally empirical models. This approach allows MARCH to simulate the behavior of all of the major reactor systems at a very fast calculation rate and very small computation cost. Thus, repetitive code runs for risk analysis activities are readily and economically performed. However, results can lack reasonability due to a lack of mechanistic models. Reference 2 contains a complete description of the MARCH code.

2.2 SCDAP/MOD0 and SCDCOMP

The SCDAP/MOD0 computer code describes the behavior of a bundle of fuel rods during extended periods of severe overheating. SCDAP simulates core disruption by modeling core heatup, core disruption and debris formation, debris heatup, and debris melting. Models in SCDAP calculate fuel and cladding temperatures, cladding oxidation, hydrogen generation, cladding ballooning and rupture, fuel and cladding liquefaction, flow and

freezing of the liquified materials, and release and transport of fission products. The code is being used to help plan severe core damage experiments, to qualify data obtained from the experiments, to aid in the determination of probabilities and uncertainties in risk assessment analyses, and to help identify the major contributors to core behavior during core uncovery accidents. The first version of the code, SCDAP/MOD0, is now in the initial assessment stage.

The calculations discussed in this paper were performed using an early version of the component analysis module of SCDAP, which is designated SCDCOMP. This module computes the behavior of single fuel rods during severel core disruptions. SCDCOMP models calculate cladding oxidation including steam starvation and hydrogen retardation effects, the liquefaction and redistribution of fuel and cladding, and rod fragmentation. The thermal-hydraulic conditions must be input by the user.

Reference 3 contains a description of the SCDAP code. Reference 4 discusses the MATPRO-11 subcode that enables the code to take into account the changes in material properties over a wide range of operating conditions.

3. PROCEDURE

Calculations of the reactor system responses were performed using the MARCH code for each of sixteen core uncovery scenarios. These calculations were performed by the Battelle Columbus Laboratories and were reported in Reference 1. The SCDCOMP code was then used to replicate these calculations for the core region. In this section, the accident scenarios will be briefly presented, then the modeling of the reactor core in the MARCH and SCDCOMP codes will be described and differences in modeling between the two codes will be discussed.

3.1 Accident Scenarios

The sixteen accident scenarios for which the computer code calculations were made were chosen earlier by the Battelle Columbus Laboratories. They were chosen to be the risk dominant and most probable initiating events for core meltdown sequences in which hydrogen burning is significant. These sequences included small, intermediate, and large break loss-of-coolant accidents (LOCAs) and transients with failure of emergency core cooling (ECC) systems. In many cases ECC was subsequently restored.

Ten of these sequences modeled a pressurized water reactor (PWR) with an ice condenser containment and typical 17 x 17 fuel bundle arrays. These sequences are:

1. Small break (5 cm diameter hole) LOCA with failure of ECC injection;

2. Small break LOCA with failure but subsequent restoration of ECC injection;

3. Small break LOCA with reduced ECC injection;

4. Small break LOCA with fuel slumping into the bottom head and failure of ECC injection;

5. Small break LOCA with failure of ECC recirculation;

6. Intermediate break (15.2 cm diameter hole) LOCA with failure of ECC injection;

7. Intermediate break LOCA with failure but subsequent restoration of ECC injection;

8. Large break LOCA with failure of ECC injection;

9. Transient with loss of power conversion, auxiliary feedwater, and ECC systems;

10. Transient with loss of power conversion, auxiliary feedwater, and ECC system, but with subsequent restoration of the ECC systems.

The remaining six sequences modeled a boiling water reactor (BWR) with a Mark III containment and typical 8 x 8 fuel bundle arrays. These sequences were:

1. Small break LOCA with failure of ECC systems;

2. Small break LOCA with failure but subsequent restoration of ECC systems;

3. Intermediate break LOCA with failure of ECC systems;

4. Intermediate break LOCA with failure but subsequent restoration of ECC systems;

5. Transient with failures of the power conversion, high pressure core spray, reactor core isolation cooling, and low pressure ECC systems;

6. Transient with failures describes in (5) above but with subsequent restoration of high pressure ECC systems.

The sequences along with the rationale for their choice are fully described in Reference 1.

3.2 Modeling in the MARCH and SCDCOMP Codes

The two computer codes used in this study have many similarities in that they both intend to model the same basic behavior phenomena in the reactor core region. However, the MARCH and SCDCOMP codes differed significantly in the modeling approaches used. The major difference was that MARCH models the behavior of the entire reactor system while SCDCOMP models only behavior of single fuel rods.

Within the reactor core, several differences existed between each code's modeling approach. The MARCH code's model of the reactor core included ten radial regions of equal volume in which the fuel, cladding, and other core materials were grouped together. In contrast, the SCDCOMP code more mechanistically models fuel rods. SCDCOMP input variables included fuel and cladding dimensions, rod pitch, rod plenum length and volume, initial rod internal gas pressure and inventory, and radial and axial power profiles. Each of the ten regions used in the MARCH code was modeled in the SCDCOMP code by a single fuel rod. The amount of zircaloy used in the SCDCOMP code included the material in fuel rod cladding and spacer grids only. In MARCH, the cladding thickness included not only the cladding and spacer grids, but also control rods, shrouds, cannisters and end pieces. Control rod and shroud models are just now becoming available in SCDCOMP.

Since the SCDCOMP code calculates rod behavior only and since the purpose of the study was to repeat the MARCH calculations as closely as possible for only the reactor core region, thermal-hydraulic boundary conditions were supplied to the SCDCOMP code from the MARCH code. These boundary conditions included heat transfer coefficients, coolant pressures and temperatures, liquid level, and steam flow rates. It was very difficult to obtain reasonable boundary conditions from the MARCH code. Several of the needed input variables for SCDCOMP were not in the printed MARCH output and others were available only at intervals of approximately five minutes. In addition,

large oscillations in the steam and hydrogen flow rates were calculated by MARCH. The oscillations were observed and noted during the assessment of MARCH[5] and were due to a subsequently discovered error[6] in the MARCH code. Because of these problems, there could be an important variation in the boundary conditions actually used by MARCH and SCDCOMP. Much care was taken to avoid these variations, but realistically some variations are expected to exit. And, analyses have shown[7] that variations in boundary conditions can significantly alter fuel rod calculations in SCDCOMP. The SCDAP/MOD0 code, which will contain the SCDCOMP module, will contain its own thermal-hydraulic models. Use of these models should provide a better estimate of fuel rod behavior and could change the results discussed below.

One further difference between the codes exists. The original intent of these analyses was to replicate the MARCH computer runs. This goal, however, could not be realized because a temperature limit is currently placed in this first version of the SCDCOMP code. Since melting of zircaloy oxide is not modeled in SCDCOMP, the code is designed to stop when temperatures reach the vicinity of 3000 K. During the early stages of SCDCOMP development, the melt limitation was not thought to be important for most expected initial uses of the code. However, for many of the scenarios analyzed in this study, the melt limitation was attained. The MOD1 version of SCDAP, to be completed in the fall of 1983, will not have this limitation.

4. RESULTS

Results of the SCDCOMP calculations of hydrogen generation rates are presented below. Comparisons of these calculations with the rates calculated by the MARCH code are made. First, results of the code comparisons for the PWR accident sequences are presented, followed by comparisons for the BWR cases. Finally, comments on the limitations of these code comparisons are made.

4.1 PWR Results

Calculations for the ten PWR scenarios described in Section 3.1 of this report and in Reference 1 were made at Battelle's Columbus Laboratories using MARCH, Version 1.1. Attempts to replicate these MARCH calculations using the MARCH, Version 1.1 code with the input variables specified in Reference 1 were successful for 9 of the 10 cases. For the one unsuccessful case (PWR transient with failure of ECC systems), a difference of approximately five minutes in the time of core uncovery and starting of core melt was observed. Boundary conditions from this MARCH calculation would not produce an accurate SCDCOMP-to-MARCH comparison. Therefore, the results below pertain only to the remaining nine accident scenarios.

Figure 1 shows hydrogen production as calculated by SCDCOMP as a function of time after reactor shutdown. The scenario for this figure was the PWR small break LOCA sequence with failure of ECC systems. The hydrogen flow rate (shown on the left axis) is represented by the solid curve and the cumulative hydrogen production (shown on the right axis) is represented by the dashed curve. Core uncovery begins at 11910 s. Generation of hydrogen begins at around 14000 s. At this time, the core was almost completely uncovered and peak cladding temperatures (as calculated by SCDCOMP) exceeded 1000 K. The Cathcart-Pawel[8] oxidation model was used for the calculations of cladding oxidation. Shortly before 15000 s, cladding temperatures in the inner core positions reached 1900 K and the Urbanic-Heidrick[9] model was used in SCDCOMP. Using this model, calculated hydrogen production is accelerated for cladding temperatures over 1850 K. This increased rate of

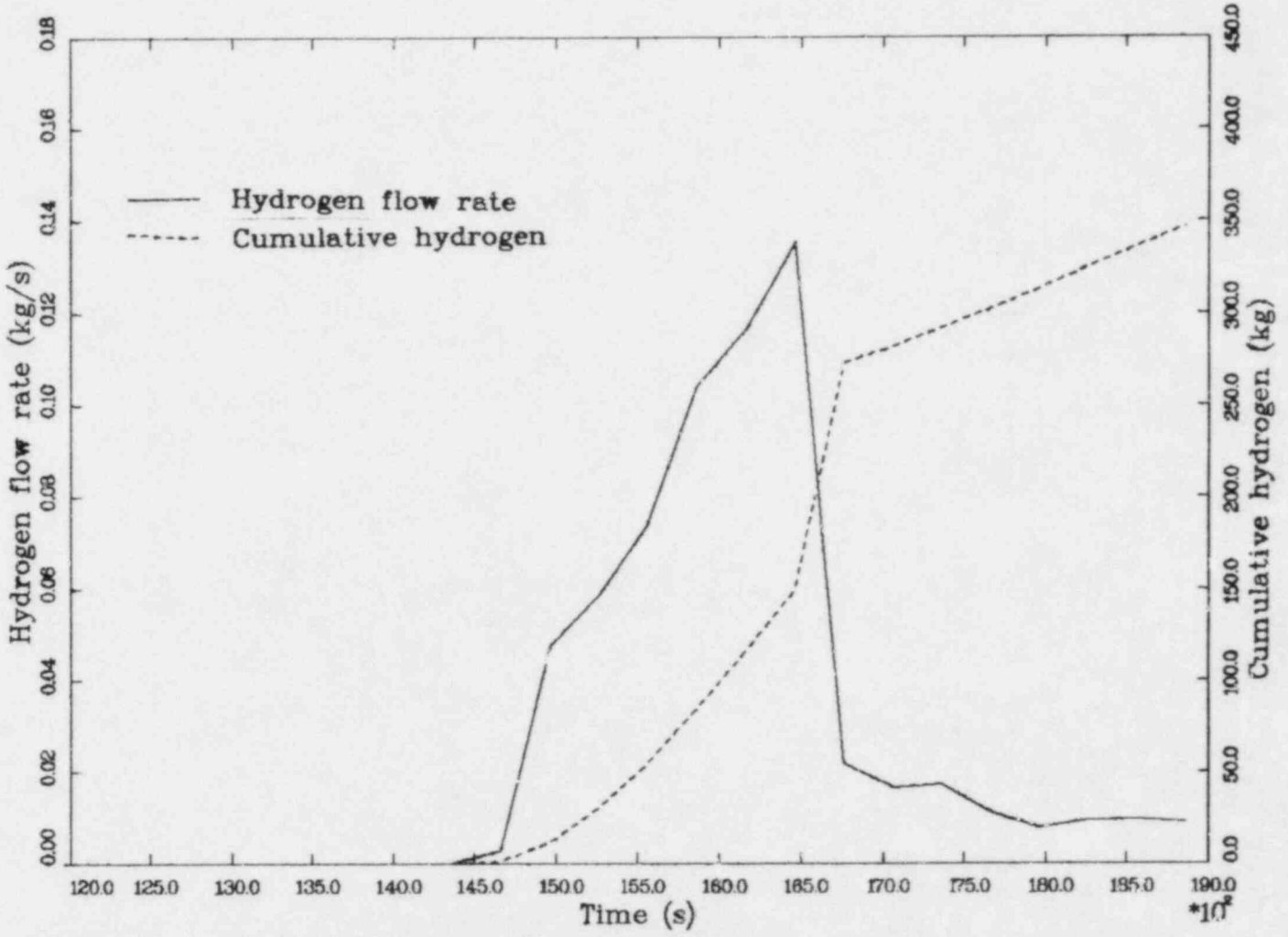

Figure 1. SCDCOMP calculations of hydrogen generation as a function of time for a PWR small break LOCA with failure of ECC injection.

hydrogen production is evident in both curves in Figure 1. At about 15500 s, the outer oxide layer of the cladding was breached and downward flow of a liquified uranium, zircaloy, and oxygen mixture began. At 16600 s, the peak cladding temperature in the outer regions of the core exceeded 1850 K and accelerated hydrogen generation began in the outer rods. At 16800 s however, the outer oxide layer of the cladding in these outer rods was breached and downward flow of a fuel-cladding mixture began. Shortly thereafter, hydrogen generation slowed dramatically as most of the cladding had flowed downward to cooler portions in both the inner and outer radii of the core. The cladding remaininig in the hotter regions of the core had already been heavily oxidized.

Figure 2 shows the SCDCOMP and MARCH calculations of total hydrogen production as a function of time after reactor shutdown for the small break LOCA with failure of ECC systems. Appendix A contains similar plots for the remaining PWR sequences. Figure 2 shows that the onset of hydrogen production as calculated by SCDCOMP is delayed by more than 10 minutes after the MARCH code showed hydrogen production to begin. The same trend was observed for the other PWR sequences. Both codes use the Cathcart-Pawel oxidation kinetics model[8] at low temperatures and this model is essentially dependent only upon temperature. The delay observed in the SCDCOMP calculations is caused primarily by two factors, both relating to temperature. First, the MARCH code uses the average rod (and therefore, other core material) temperature while the SCDCOMP code uses the average cladding oxide layer temperature. Second, different cladding heatup rates were probably calculated. Although the thermal-hydraulic boundary conditions were calculated by MARCH, and were input into SCDCOMP, they were only available at intervals of approximately five minutes. The SCDCOMP code then used linear interpolation to calculate water level, steam flow rates, and heat transfer coefficients at times between these five minute spans. Therefore, core uncovery could commence at different times in the two code calculations. For this reason, at any given time, essentially different cladding heatup rates were most likely used in the two codes. Therefore, the time parameter was deemed to have little significance in the code comparisons.

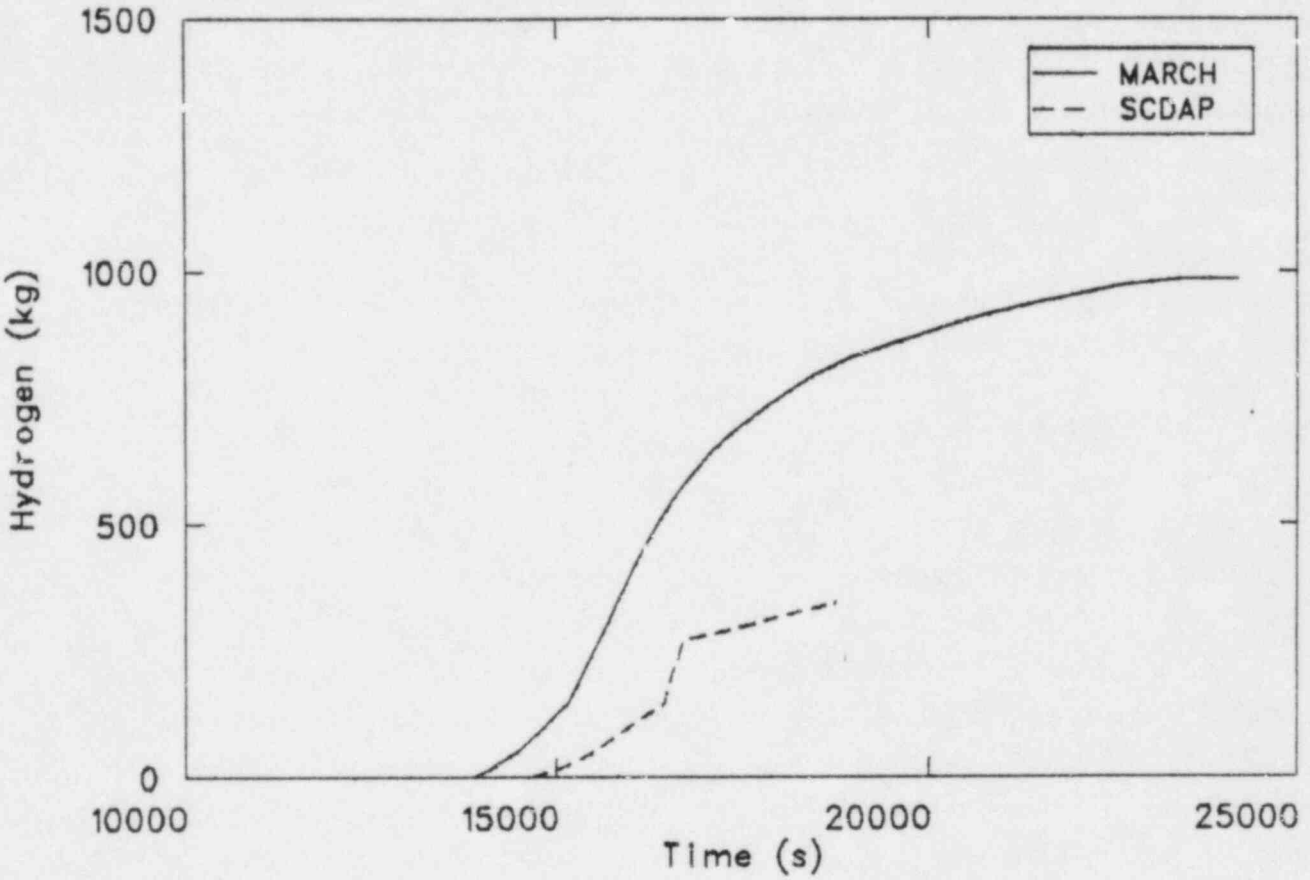

Figure 2. SCDCOMP and MARCH calculations of hydrogen production versus time for a PWR small break LOCA with failure of ECC injection.

Since oxidation kinetics models are heavily dependent upon temperature, comparisons of hydrogen generation rates as calculated by the two codes were made as functions of temperature for those scenarios in which there was no time-dependent influence (such as ECC injection) on temperature. Figure 3 shows the ratio of the hydrogen generation rate calculated by SCDCOMP to that calculated by MARCH as a function of cladding temperature. The scenarios represented in this figure are those in which ECC was not injected or was continuously injected at a degraded level. Two trends can be noted in this plot. First, all curves increase until a maximum ratio is attained between 2100 and 2300 K, and then the ratios decrease. Second, the curves separate naturally into three groups (upper, middle, and lower ratios) corresponding to the cladding temperature rate of increase, or heating rate. These two trends will be discussed below.

The maximum ratio shown for each of the curves divides the figure into two distinct regions; that is, the region with temperatures less than 2200 K and that with temperatures greater than 2200 K. In both SCDCOMP and MARCH, the Cathcart-Pawel[8] model is used. However, for temperatures above 1850 K, the Urbanic-Heidrick model[9] is used in SCDCOMP. This second model accelerates oxidation and causes the hydrogen generation rate to increase relative to the MARCH calculated rate. Above 2200 K, the rate calculated by SCDCOMP decreases and becomes smaller than the MARCH rate because SCDCOMP modeling allows downward flow of a molten mixture of zircaloy, uranium, and oxygen. This flowing removes the source of oxidation from the hotter regions of the core and thereby decreases the ratio of hydrogen generation by SCDCOMP. The MARCH calculation, on the other hand, artificially held material in the upper, hotter portions of the core until 100% of this material had melted, causing a larger oxidation rate than was calculated by SCDCOMP.

The three groups shown in Figure 3 correspond to three different cladding heating rates resulting from different scenarios. The upper curve was obtained for a small break LOCA scenario with continuously injected ECC. The rate of cladding temperature rise was largest for this scenario, since water was always available in the core for oxidation. The middle curves represent large and medium break LOCAs with no ECC. The heating rate for these scenarios was smaller than that previously mentioned. The smallest

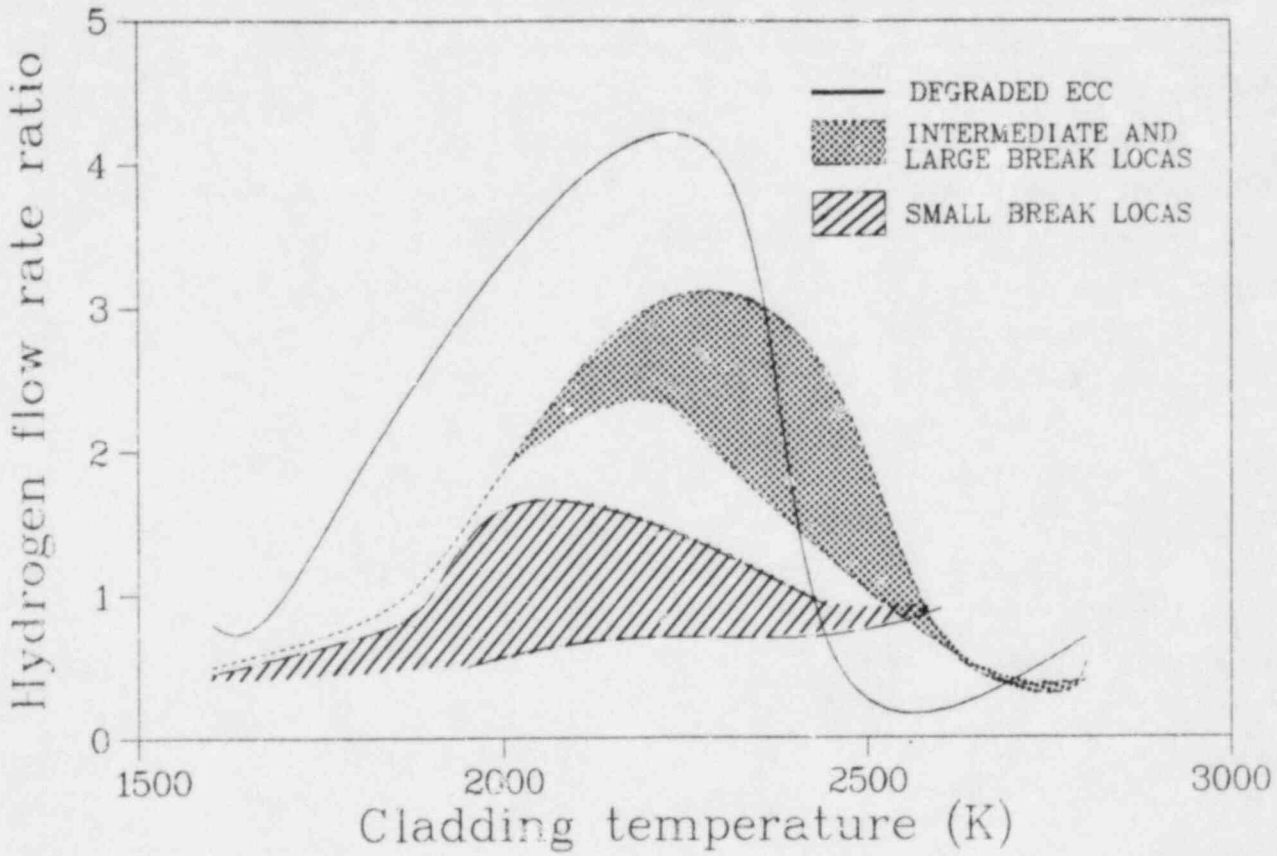

Figure 3. Ratio of SCDCOMP to MARCH hydrogen generation rates versus cladding surface temperature.

heating rate was calculated for the small break LOCAs represented in the lower portion of the figure. The slower the temperature rise in the cladding, the thicker the oxide layer that is formed at low temperatures. With thicker oxide layers, less influence would be felt by the rods when an increased oxidation rate or a downward flow of zircaloy is initiated.

In some of the PWR scenarios, ECC was injected after core uncovery. This increase in the amount of steam available for oxidation caused an 80 to 1500% increase in the hydrogen generation rates calculated by SCDCOMP. Figure 4 shows an example of a scenario in which ECC was injected after core uncovery. The figure represents the small break LOCA with failure but subsequent restoration of ECC injection. Cumulative hydrogen generation for both the MARCH and SCDCOMP calculations are shown. Core uncovery was initiated at 12240 s and ECC was injected at 15900 s. At the time of ECC injection, the rate of hydrogen production by SCDCOMP increased by about 1500%. However, little change was noted in the hydrogen production rate calculated by MARCH. The increased hydrogen generation rates continued in all cases until the core was sufficiently cooled by the rising water or until downward flow of liquid core material had displaced enough zircaloy to cause oxidation to slow or to cease altogether or until the SCDCOMP melt limitation was reached. In contrast, MARCH calculations showed a relative insensitivity to ECC injection. An increase in the hydrogen generation rates calculated by MARCH was observed in only one of the three cases.

4.2 BWR Results

Calculations were made for each of the six BWR sequences, as described in Section 3 and Reference 1, using both the MARCH and the SCDCOMP code. SCDCOMP calculations of the hydrogen generation rate and cumulative hydrogen production for the BWR intermediate break LOCA with failure of ECC systems is shown in Figure 5. The core was uncovered at 2160 s and hydrogen generation was calculated to begin shortly after 2700 s. The increased rate of hydrogen generation seen at about 3100 s was due to use of the Urbanic correlation since temperatures reached 1850 K at about that time. Shortly before 3400 s, the outer oxide layer was breached and downward flow of a fuel-cladding mixture began, causing the hydrogen generation rate to

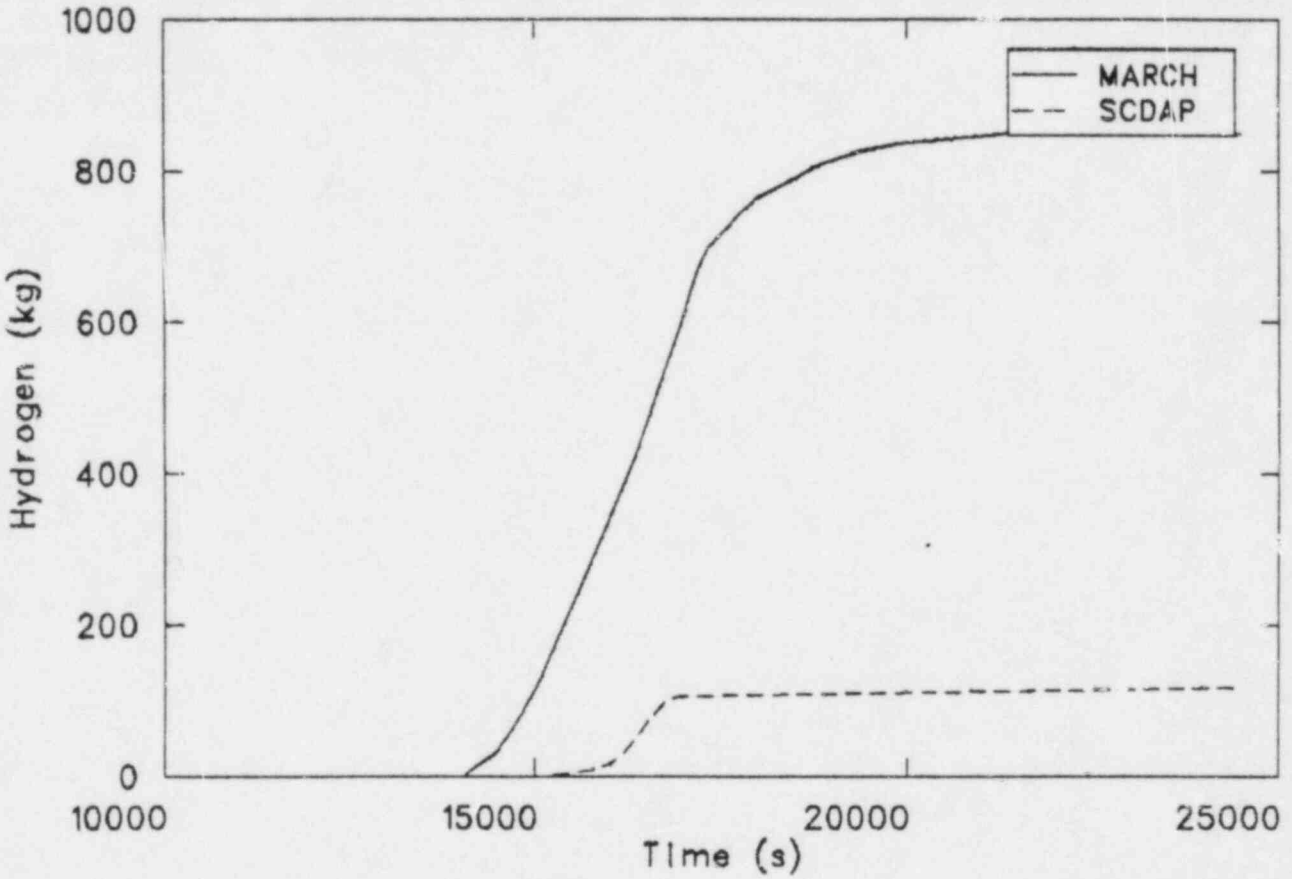

Figure 4. SCDCOMP and MARCH calculations of hydrogen production versus time for a PWR small break LOCA with failure but subsequent restoration of ECC injection.

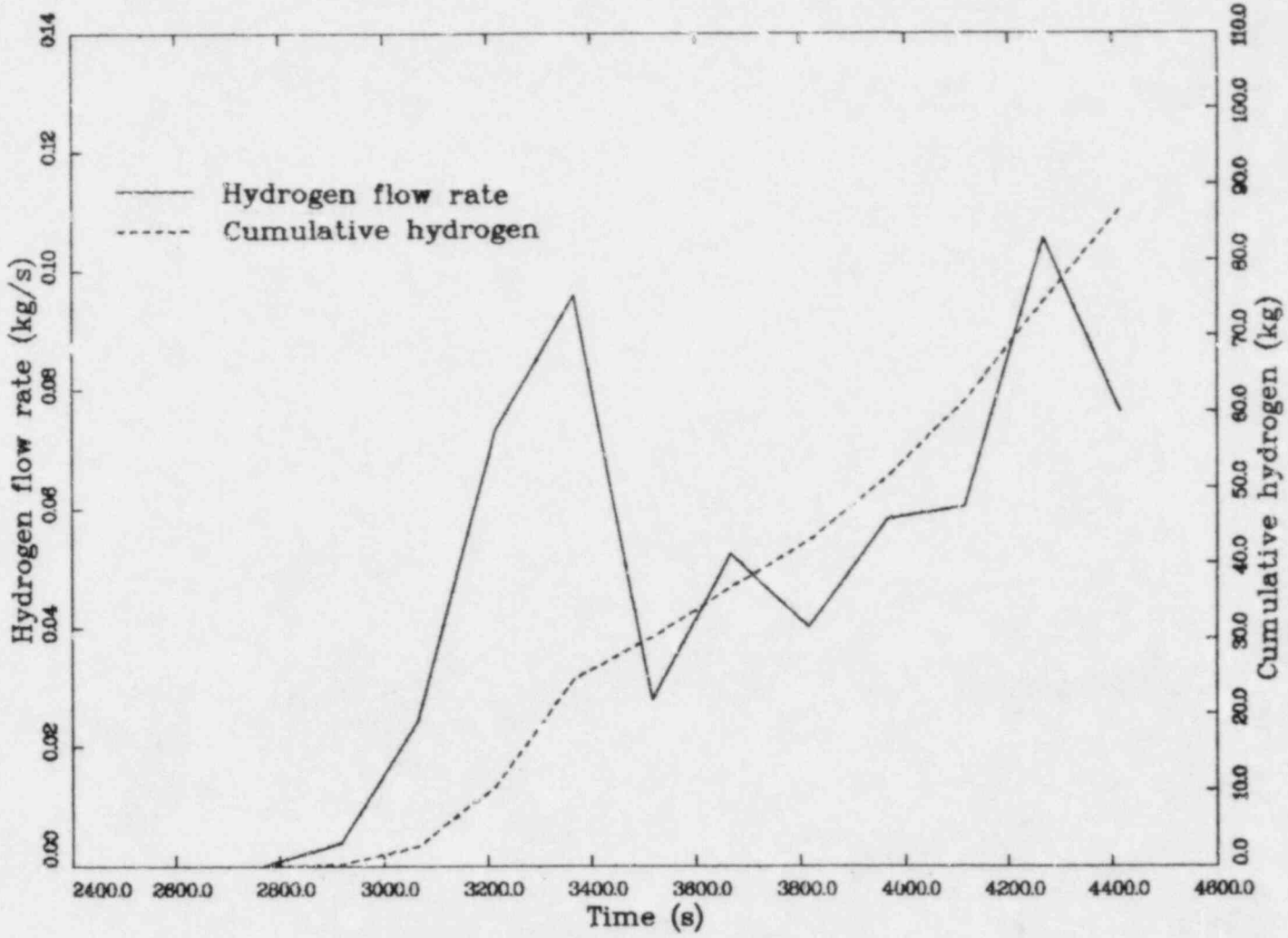

Figure 5. SCDCOMP calculations of hydrogen generation as a function of time for a BWR intermediate break LOCA with failure of ECC systems.

decrease. The later rate increase seen at about 4100 s was caused by the outer rods reaching high enough temperatures to oxidize rapidly and contribute significantly to the hydrogen flow.

Figure 6 shows a comparison of the SCDCOMP and MARCH calculations of cumulative hydrogen production as a function of time for a small break LOCA in a BWR. Similar plots for the remaining BWR sequences can be found in the Appendix. As for the PWR scenarios, an offset in the time of beginning of hydrogen production between the two codes is seen. However, for the BWR sequences, the SCDAP calculation of the onset of hydrogen production was earlier than the MARCH calculation. The opposite was observed for the PWR sequences. Again this can be attributed to temperature. The heatup rate in the MARCH calculation was probably slower because the coolant froth above the liquid water was deeper for the BWR than the PWR sequences. The compressed liquid level was input into the SCDCOMP code, as demanded by the SCDCOMP input requirements. The higher level of coolant in the MARCH calculations would cause higher portions of the fuel rods to be cooler in MARCH than in SCDCOMP resulting in a later heatup and consequently a later onset of cladding oxidation in MARCH than SCDCOMP.

An important contributor to the differences in the hydrogen production calcuations performed by SCDCOMP and MARCH is the mass of zircaloy in the core. One of the input variables for the MARCH code is the cladding thickness. This input parameter effectively groups the mass of cladding, spacers, end pieces, and other zircaloy components in the core into one input value. The cladding thickness input for the BWR rods accounted for more than twice the mass of zircaloy as would be found in the cladding alone. Therefore more than twice the material available for oxidation was used in the MARCH code as in the SCDCOMP code for BWR rods. (About 15% more zircaloy was used in MARCH for the PWR scenarios.) Although the usage of the correct amount of zircaloy would result in a correct estimate in MARCH of the total hydrogen generated due to complete consumption of zircaloy, altering the fuel rod cladding thickness invalidates the use of standard oxidation rate equations. As a consequence, the rate of hydrogen generation predicted by MARCH will be distorted. On the other hand, the models of control rods and shrouds, which will soon be available in SCDCOMP, will make accurate use of the oxidation rate equations, if realistic boundary conditions are supplied.

not believed that the conclusions of the study will change significantly. The limited assessment of the SCDCOMP code that has been done to date supports the general trends discussed in this report.

5. CONCLUSIONS

The fuel rod behavior portion of the MARCH calculations was replicated using the SCDCOMP module of the SCDAP code. The rate and cumulative hydrogen production calculations by the two codes were compared. As a result of the study reported here, the following conclusions have been reached:

1. Hydrogen generation calculations are sensitive to two mechanistic models affecting cladding oxidation that are present in SCDAP but absent in MARCH, Version 1.1.

   Differences between the hydrogen generation calculations performed using the two codes are primarily due to two models that are included in SCDCOMP but not in MARCH. The first model calculates accelerated zircaloy oxidation at high temperatures and the second calculates downward relocation of a mixture of liquefied cladding and fuel. These models result in a trend of increasing oxidation rates at high temperatures until the flow of the liquefied cladding and fuel commences. Because of this flow to cooler core regions, oxidation rates decrease rapidly.

2. The quantity and rate of hydrogen generation calculated by SCDCOMP is scenario dependent.

   This trend was noted by viewing plots of hydrogen generation for all scenarios that were modeled. Scenarios with slower heatup rates showed a slower rate of hydrogen production than scenarios with faster heatup rates.

3. SCDCOMP is more sensitive than MARCH, Version 1.1, to increased steam flow due to ECC injection.

   The increase in steam available for oxidation caused a significant increase in the hydrogen generation rates calculated by SCDCOMP, while MARCH calculations showed a relative insensitivity to ECC injection.

4. SCDCOMP modeling of fuel rods allows more accurate use of oxidation kinetics models.

   The SCDCOMP code models fuel rods and their geometries while the MARCH code groups fuel, cladding, and other core materials together. In the MARCH code, zircaloy from core structure and other non-fuel rod components is added to the original fuel rod cladding. Altering the fuel rod cladding geometry invalidates the use of standard oxidation rate equations, which are dependent upon rod surface area and zircaloy thickness.

The largest problem encountered in the study was the difficulty in obtaining boundary conditions from the MARCH code. There could be large variations in the boundary conditions used by MARCH and SCDCOMP. When the best-estimate thermal-hydraulic models in SCDAP are linked with the SCDCOMP models, the results described above could be altered.

6. RECOMMENDATIONS

In this section, recommendations are given on how to use the results of this study in conjunction with the results of the MARCH calculations for purposes of future NRC rulemaking. Also, recommendations for future analyses using SCDAP are proposed.

Two options for the steam and hydrogen flow rates into the containment for the purpose of investigating proposed hydrogen mitigation systems are given in Reference 1. In using these options, two points should be kept in mind. First, experimental evidence has shown that hydrogen generation rates increase when cladding temperatures exceed 1850 K. When analyses using the MARCH code are made, and cladding temperatures are in the range of 1850 K to about 2300 K, hydrogen generation rates as calculated by MARCH could be too small. Second, MARCH does not account for changes in the oxidation reaction surface area due to cladding swelling, ballooning, rupture, and, particularly to downward flow of cladding material to cooler core regions. The rate of the oxidation reaction as calculated by MARCH could be too large when cladding temperatures exceed 2300 K. These trends can be seen in Figure 3 of this report and should therefore be taken into account when using hydrogen calculations performed by the MARCH code. The hydrogen production rates calculated by the MARCH code should be adjusted by the amount indicated in Figure 3.

As mentioned previously, changes in the boundary conditions can significantly affect the SCDCOMP calculations. It is therefore recommended that several of these calculations be redone using thermal-hydraulic boundary conditions obtained from a best estimate system code. SCDAP/MOD0 will contain such a subcode to make these thermal-hydraulic calculations. It is also recommended that SCDAP/MOD0 be used to calculate hydrogen production for very severe accident scenarios resulting in very large amounts of hydrogen production to provide an upper bound of hydrogen flow into reactor containments.

7. REFERENCES

1. P. Cybulskis, A Method for the Analysis of Hydrogen and Steam Releases to Containment During Degraded Core Cooling Accidents, NUREG/CR-2540, BMI-2090, February 1982.

2. R. O. Wooten and H. I. Avci, MARCH (Meltdown Accident Response Characteristics) Code Description and User's Manual, NUREG/CR-1711, BMI-2064, October 1980.

3. C. M. Allison et al., Severe Core Damage Analysis Package (SCDAP) Code Conceptual Design Report, EGG-CDAP-5397, April 1981.

4. D. L. Hagrman, G. A. Reymann, R. E. Mason (eds.), MATPRO-Version 11 (Revision 2): A Handbook of Materials Properties for Use in the Analysis of Light Water Reactor Fuel Rod Behavior, NUREG/CR-0497, TREE-1230, Rev. 2, August 1981.

5. J. B. Rivard et al., Interim Technical Assessment of the MARCH Code, NUREG/CR-2285, SAND81-1672, R3, November 1981.

6. F. E. Haskin and C. J. Shaffer, "Impact of Meltdown Accident Modeling Developments on PWR Analysis," International Meeting on Thermal Nuclear Reactor Safety, Chicago, Illinois, August 29-September 2, 1982.

7. C. M. Alison, T. M. Howe, and G. P. Marino, "Initial SCDAP Predictions of the TMI-2 Event," Tenth Water Reactor Safety Research Information Meeting, Washington, D.C., October 12-15, 1982.

8. J. V. Cathcart, Quarterly Progress Report on the Zirconium Metal-Water Oxidation Kinetics Program Sponsored by the NRC Division of Reactor Safety Research for October-December 1976, ORNL/NUREG/TM-87, February 1977.

9. V. F. Urbanic and T. R. Heidrick, "High Temperature Oxidation of Zircaloy-2 and Zircaloy-4 in Steam," Journal of Nuclear Materials, 75, 1978, pp. 251-261.

APPENDIX A

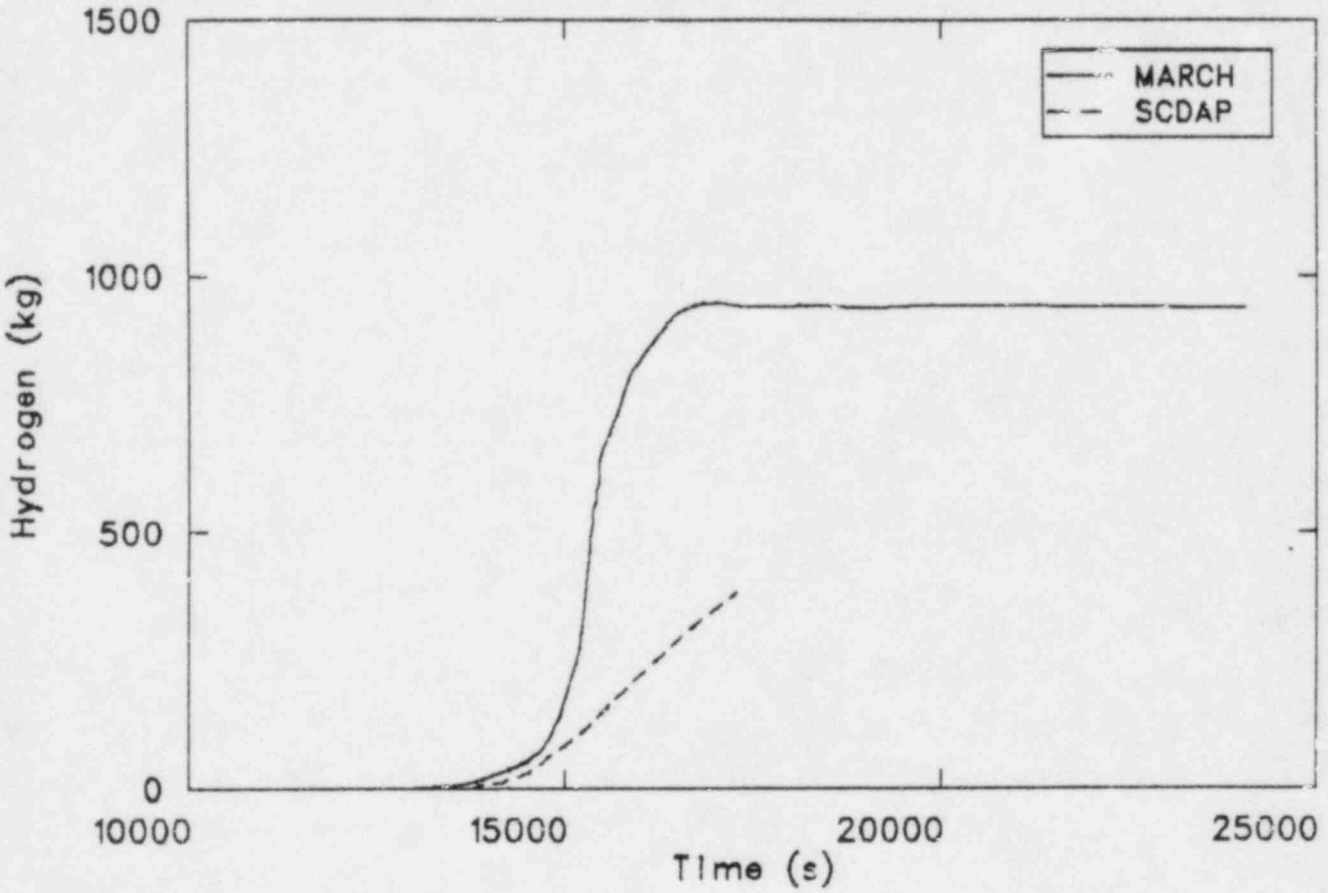

Figure A-1. SCDCOMP and MARCH calculations of hydrogen production versus time for a PWR small break LOCA with reduced ECC injection.

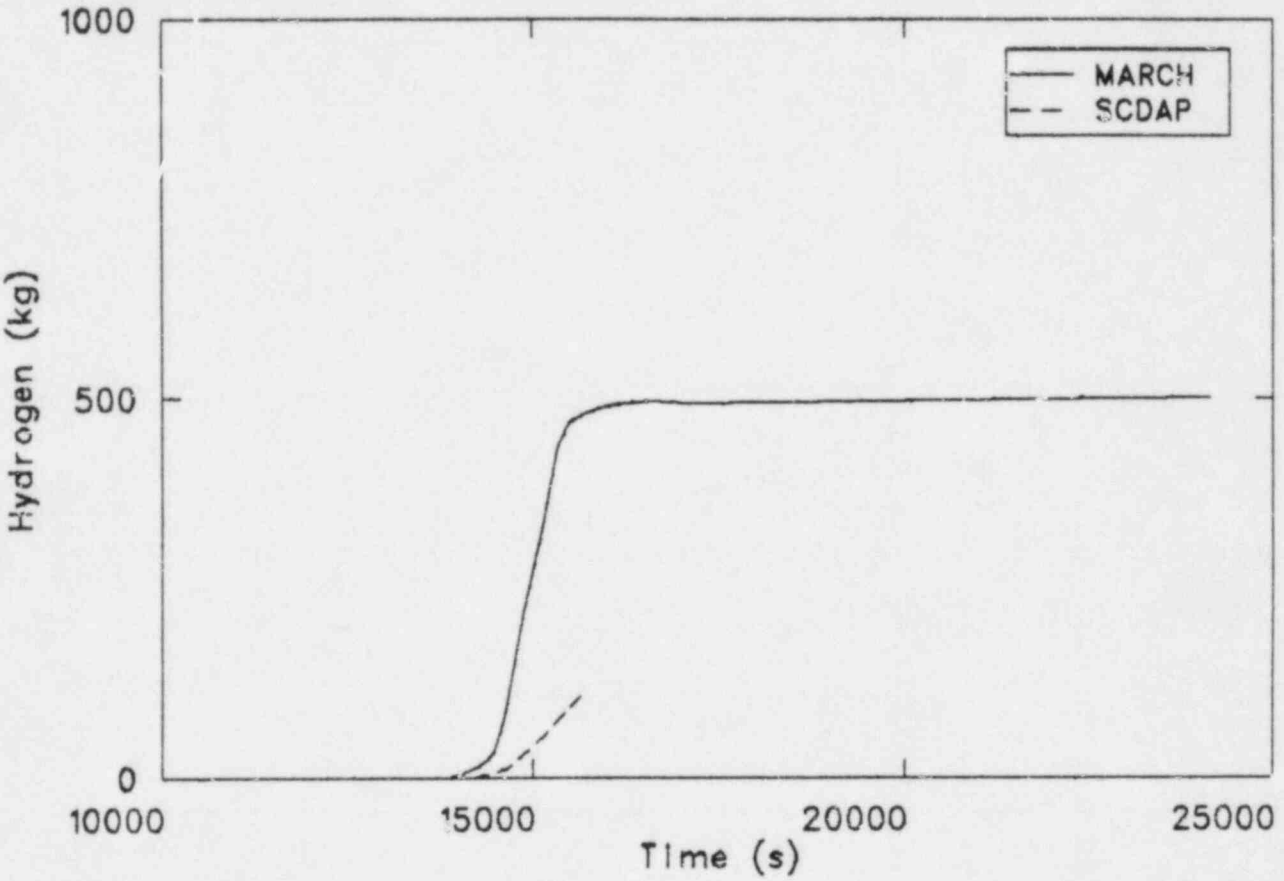

Figure A-2. SCDCOMP and MARCH calculations of hydrogen production versus time for a PWR small break LOCA with fuel slumping into the bottom head and failure of ECC injection.

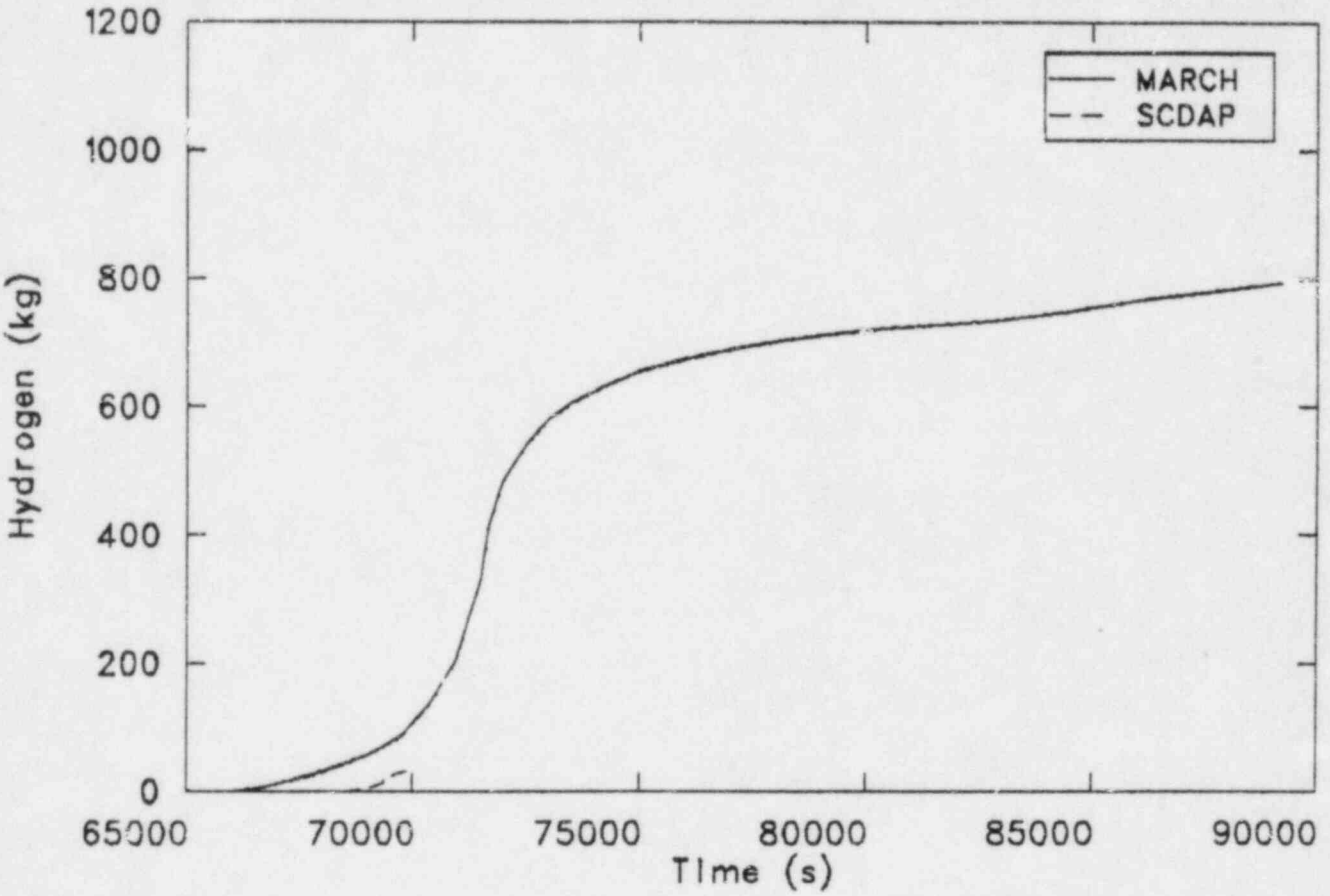

Figure A-3. SCDCOMP and MARCH calculations of hydrogen production versus time for a PWR small break LOCA with failure of ECC recirculation.

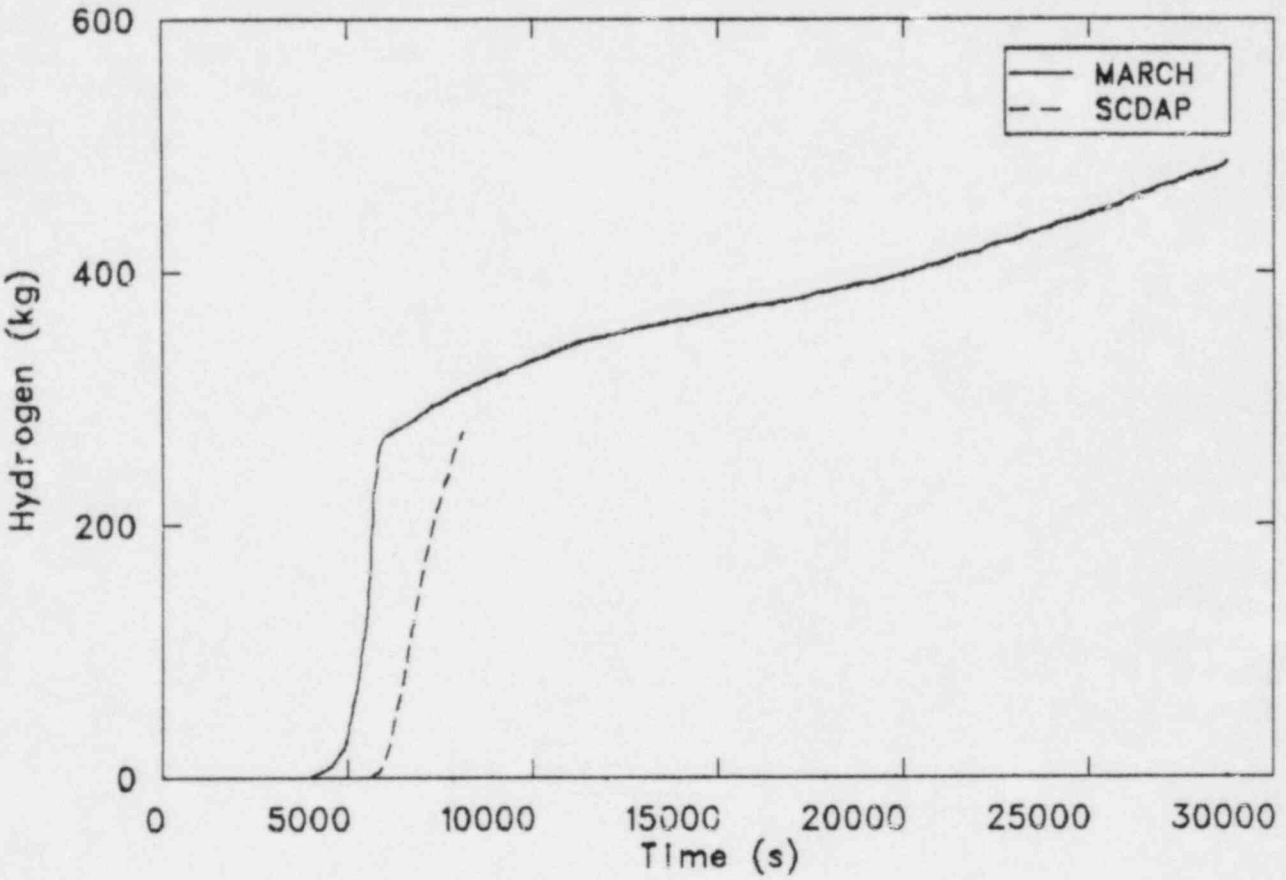

Figure A-4. SCDCOMP and MARCH calculations of hydrogen production versus time for a PWR intermediate break LOCA with failure of ECC injection.

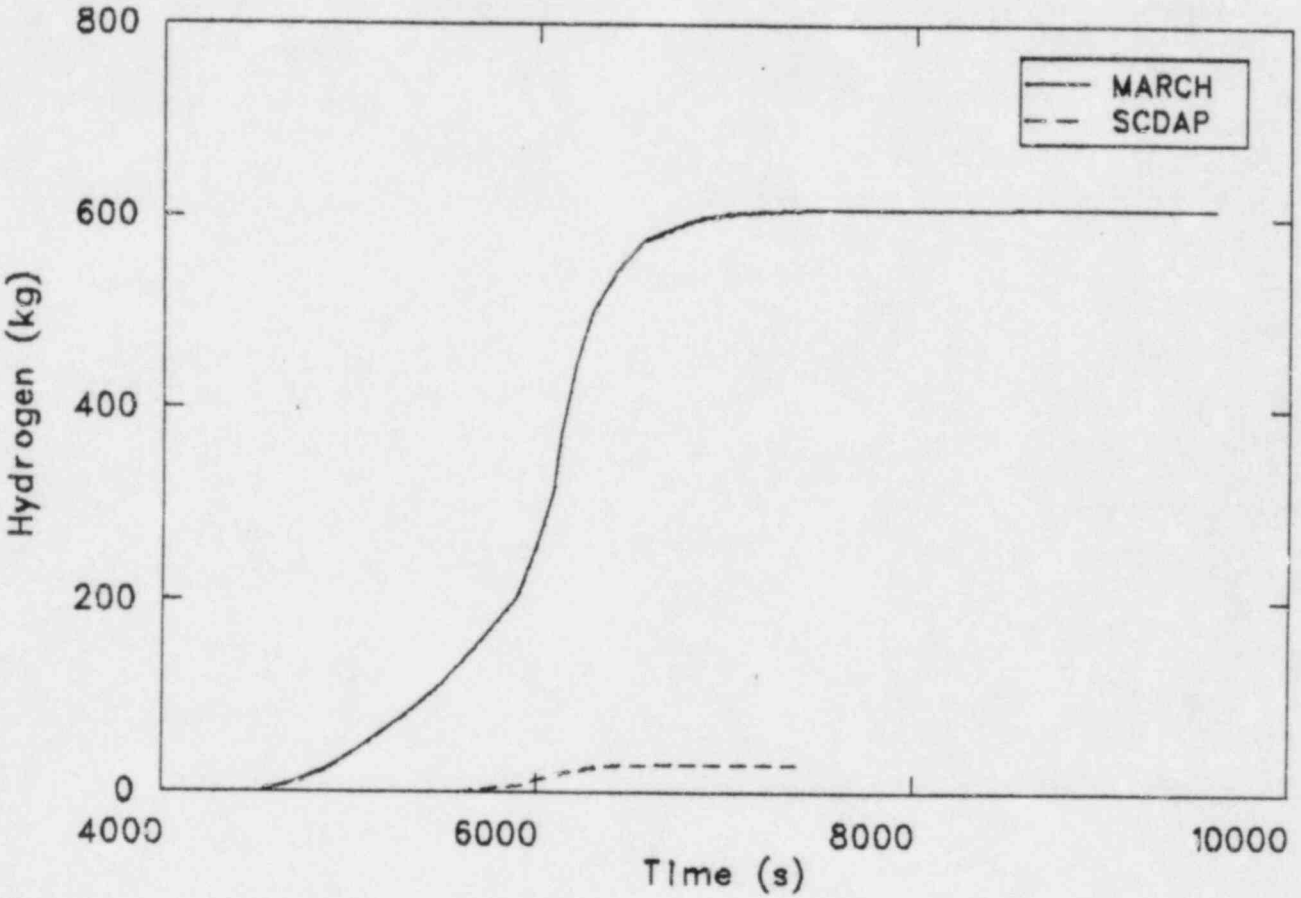

Figure A-5. SCDCOMP and MARCH calculations of hydrogen production versus time for a PWR intermediate break LOCA with failure but subsequent restoration of ECC injection.

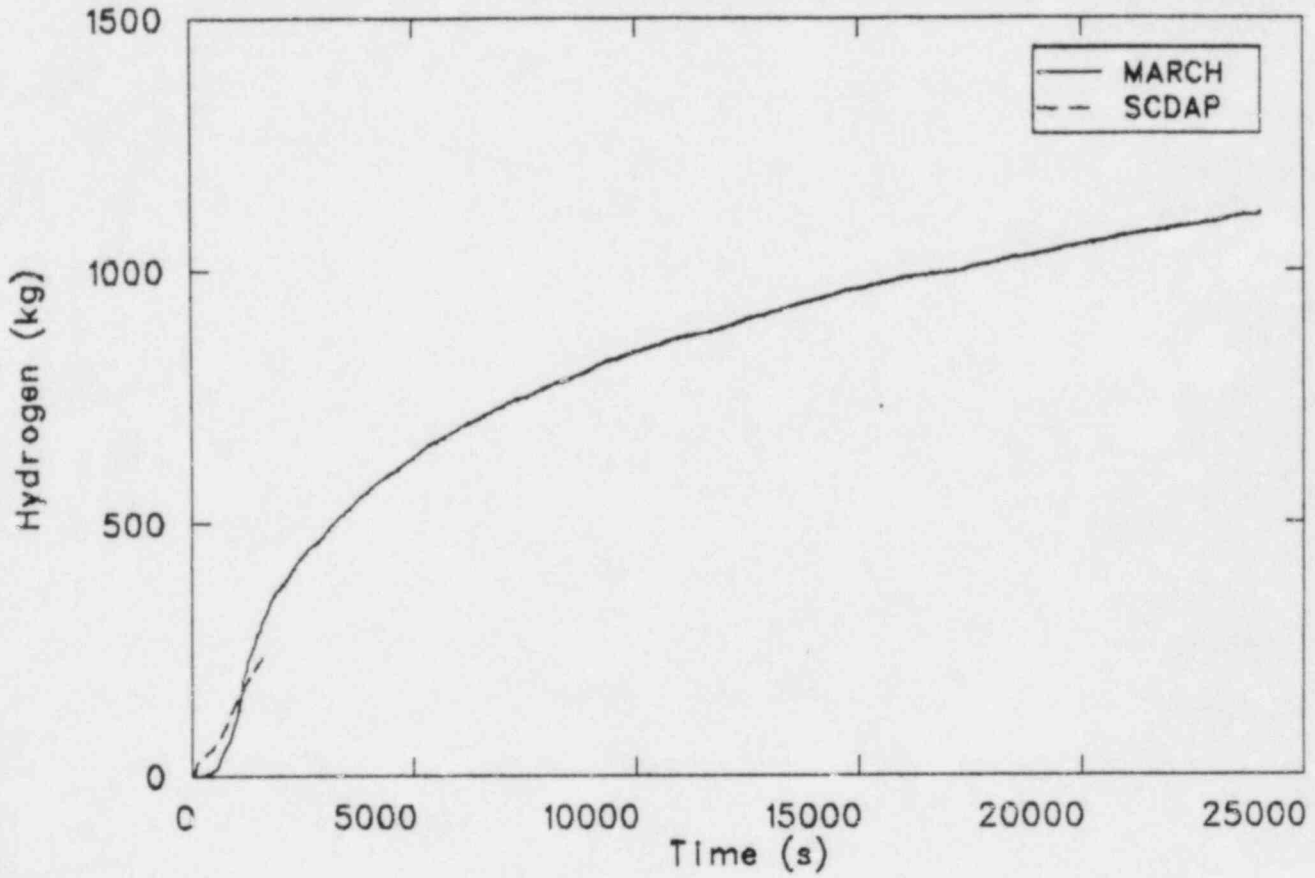

Figure A-6. SCDCOMP and MARCH calculations of hydrogen production versus time for a PWR large break LOCA with failure of ECC systems.

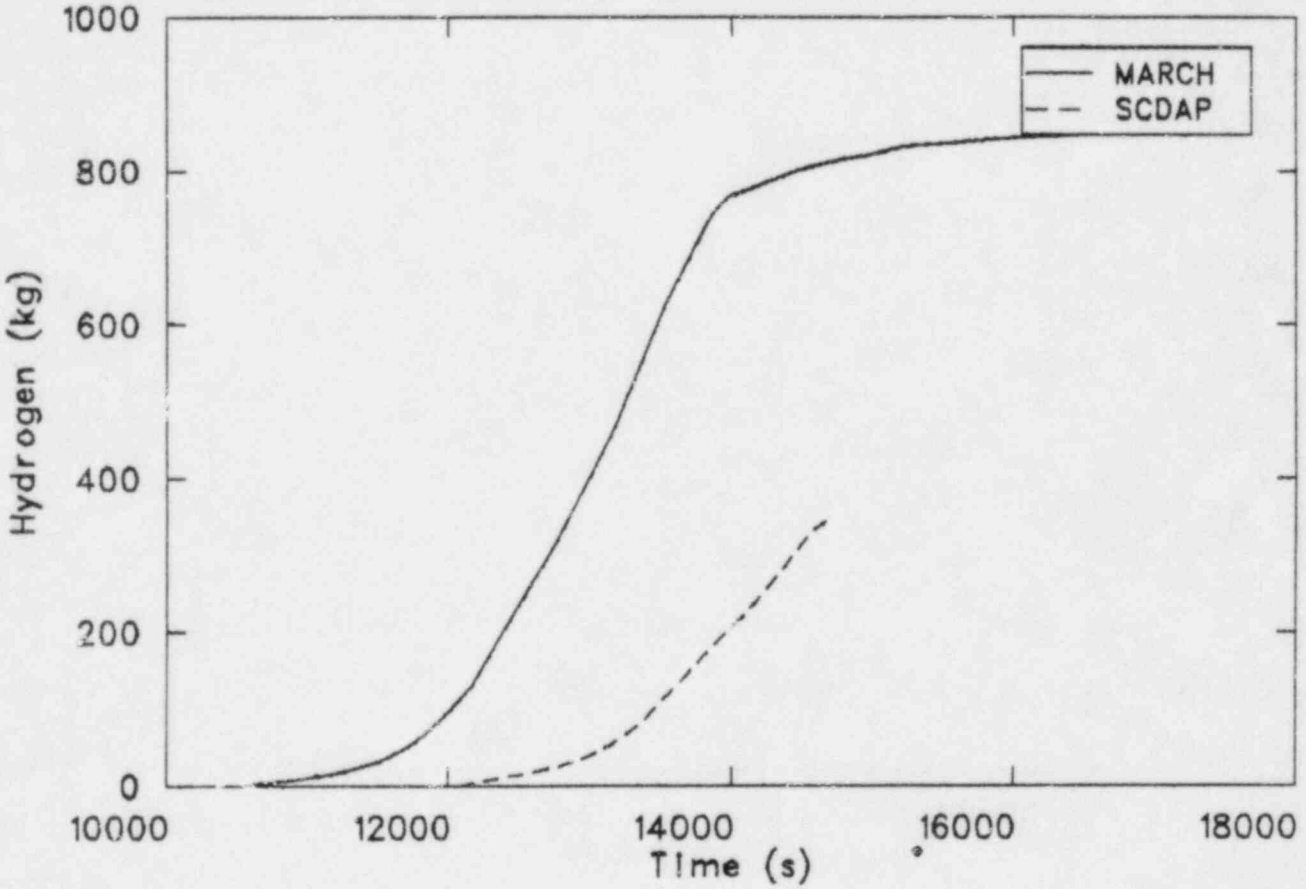

Figure A-7. SCDCOMP and MARCH calculations of hydrogen production versus time for a PWR transient with loss of power conversion, auxiliary feedwater and ECC systems, but with subsequent restoration of the ECC systems.

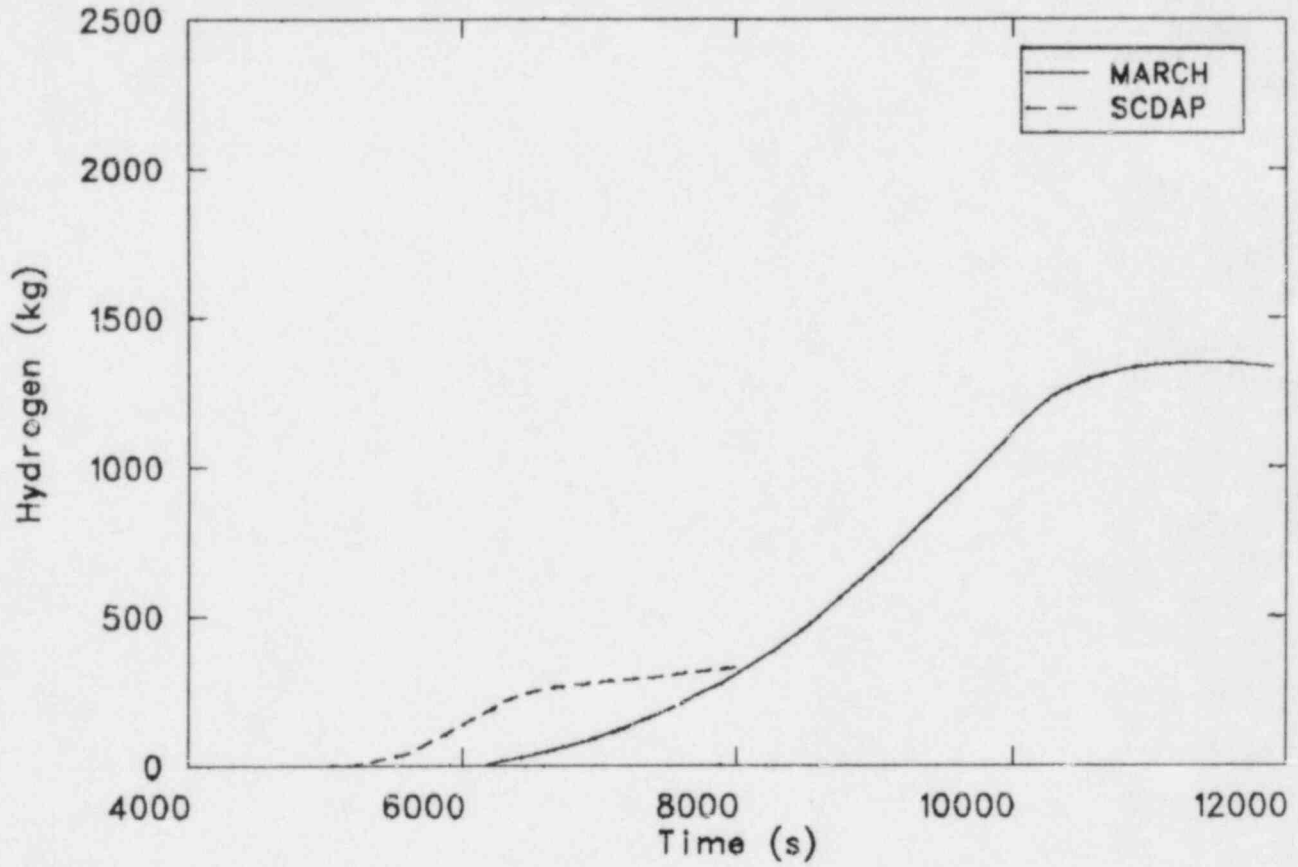

Figure A-8. SCDCOMP and MARCH calculations of hydrogen production versus time for a BWR small break LOCA with failure but subsequent restoration of the ECC systems.

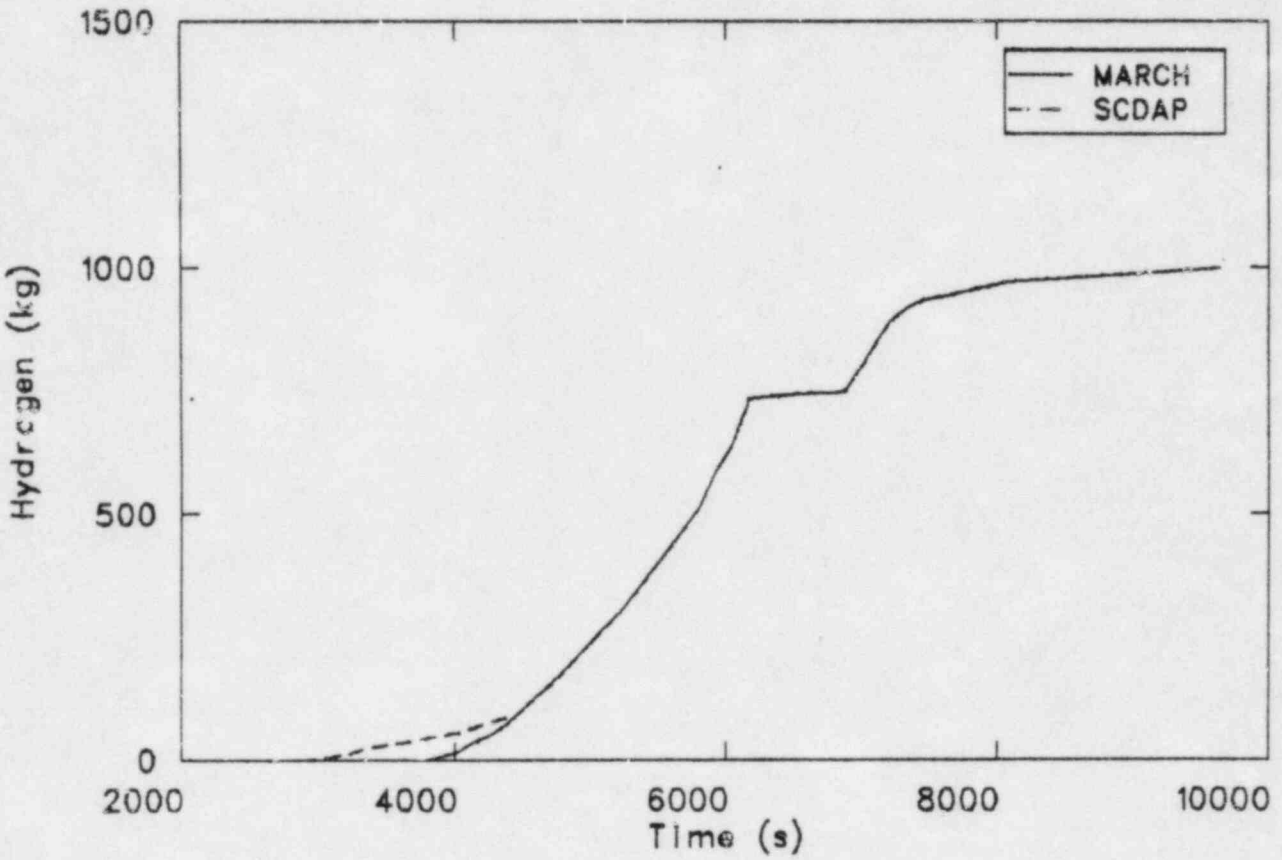

Figure A-9. SCDCOMP and MARCH calculations of hydrogen production versus time for a BWR intermediate break LOCA with failure of ECC systems.

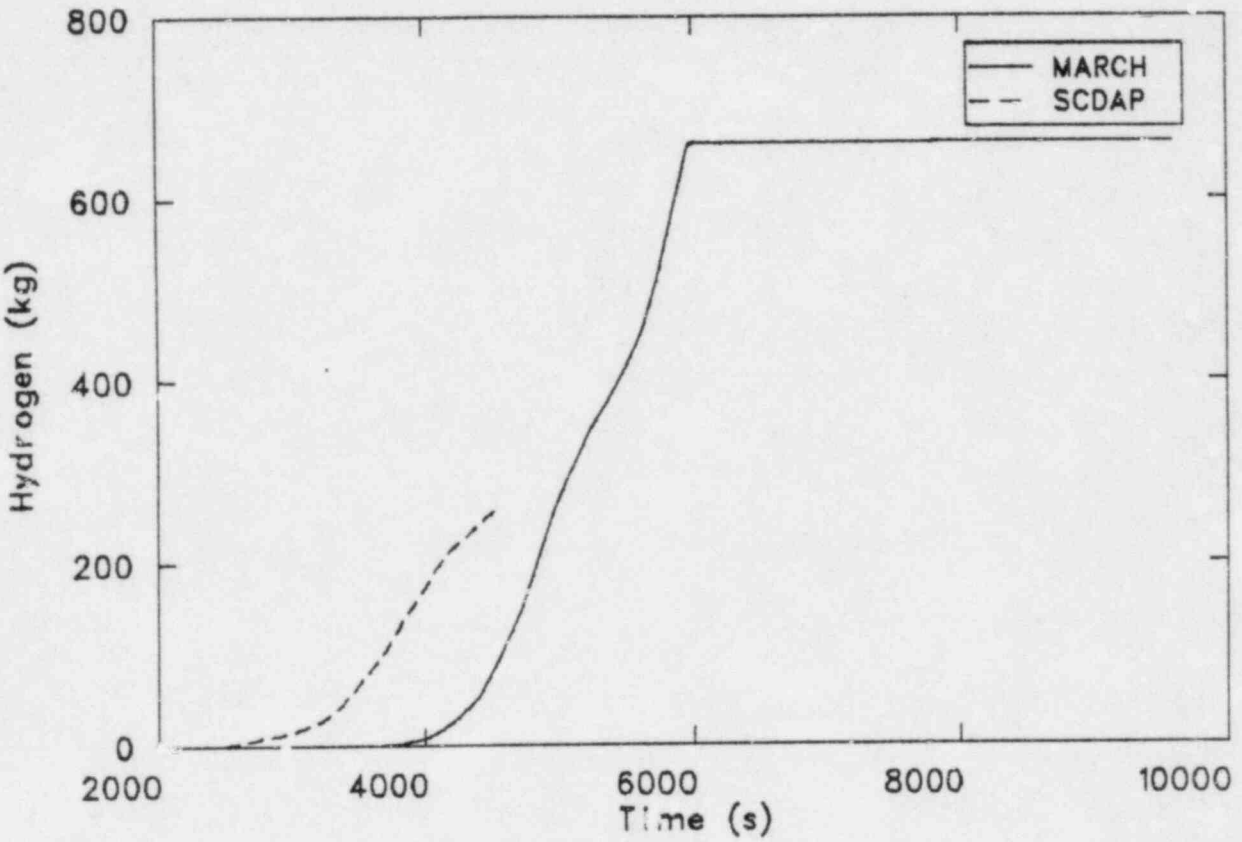

Figure A-10. SCDCOMP and MARCH calculations of hydrogen production versus time for a BWR intermediate break LOCA with failure but subsequent restoration of ECC systems.

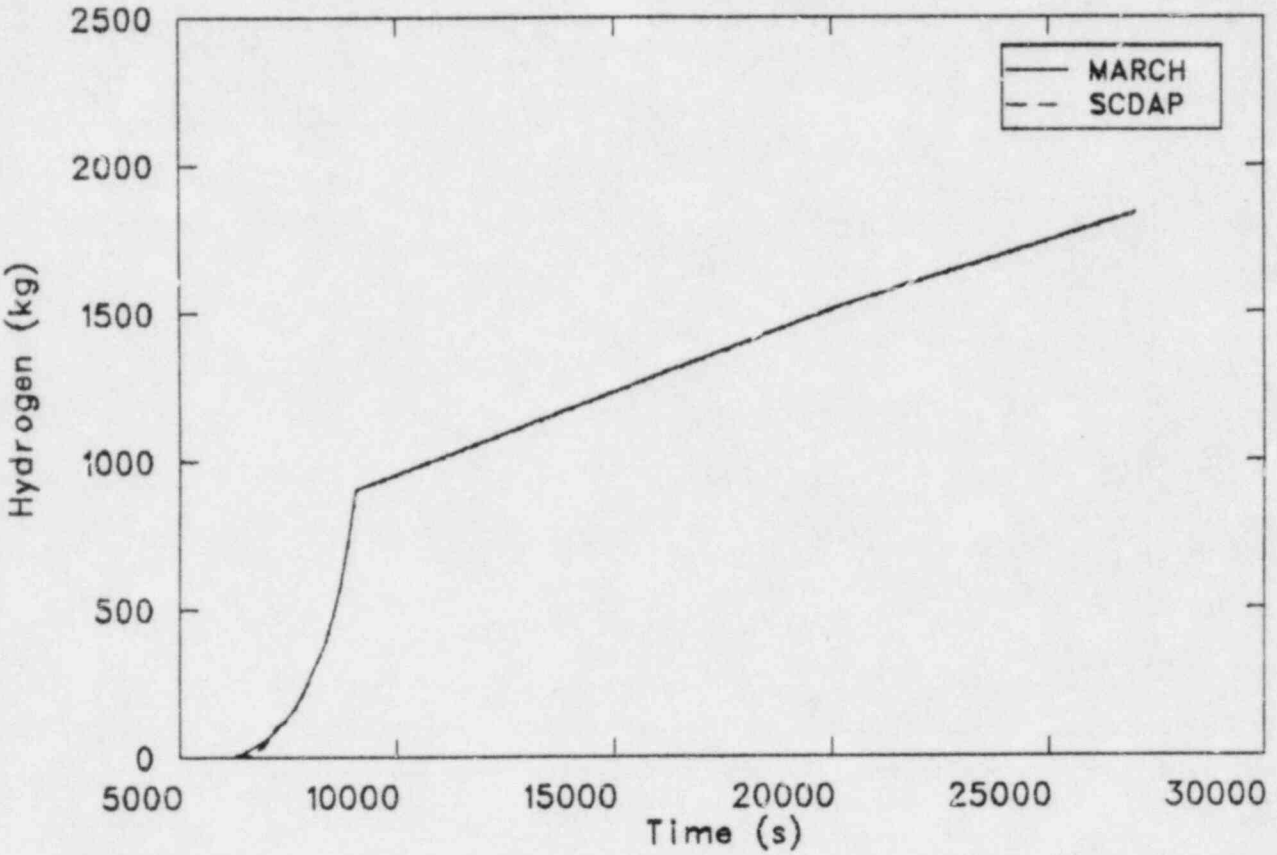

Figure A-11. SCDCOMP and MARCH calculations of hydrogen production versus time for a BWR transient with failures of power conversion, high pressure core spray, reactor core isolation cooling, and low pressure ECC systems.

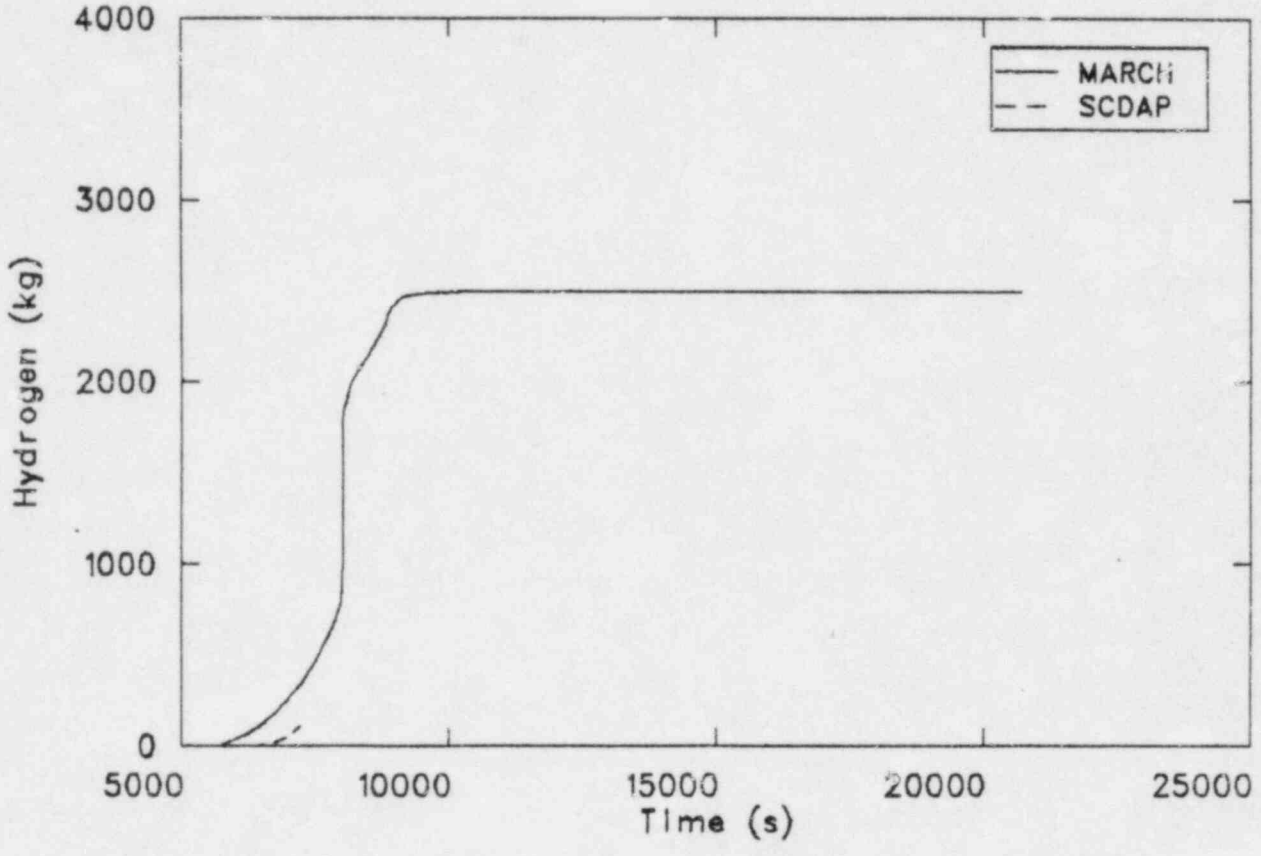

Figure A-12. SCDCOMP and MARCH calculations of hydrogen production versus time for a BWR transient with failures of power conversion, high pressure core spray, reactor core isolation cooling, and low pressure ECC systems, but with subsequent restoration of the latter.